VOLUME 11 NOMOR 2 DECEMBER 2024 ISSN 2548 – 611X

JURNAL
BIOTEKNOLOGI & BIOSAINS INDONESIA

Homepage Jurnal: http://ejournal.brin.go.id/JBBI/index

STUDY OF ANTI-BACTERIAL AND ANTI-INFLAMMATORY PROPERTIES OF INDONESIA'S FLORA BIODIVERSITY AS DRUG CANDIDATES FOR DIABETIC ULCER THROUGH *IN SILICO* AND *IN VITRO* APPROACH

Kajian Sifat Anti Bakteri dan Anti Inflamasi Keanekaragaman Hayati Flora Indonesia sebagai Kandidat Obat Ulkus Diabetik melalui Pendekatan *In Silico* dan *In Vitro*

Cecilia Tiffanny[1], Aurelia Regina[2], Davin Handreas Chen[1], Margaretha Maria Rosyati[1]
[1]Santa Laurensia Senior High School, South Tangerang, Banten 15325, Indonesia
[2] Faculty of Medicine, Airlangga University, Surabaya, Indonesia
*Email: m.rosyati@santa-laurensia.sch.id

ABSTRACT

This study is driven by the substantial increase in the number of diabetes mellitus patients, which is projected to triple by 2030 and the immense potential of Indonesia's extensive biodiversity. Diabetic ulcers represent one of the most common complications stemming from uncontrolled diabetes mellitus. Therefore, this research aims to determine the therapeutic potential of Indonesian biodiversity for diabetic ulcers, focusing on the anti-bacterial and anti-inflammatory properties of secondary metabolite derivatives, employing both in silico and in vitro approaches. Initially, the research employed an in silico approach, conducting molecular docking and molecular dynamics simulations on reference ligands obtained from the 6KVS receptor for Staphylococcus aureus bacteria and the 5KIR for the COX-2 protein. Molecular docking was performed for 18 secondary metabolite derivative test compounds using Autodock Vina, followed by molecular dynamics simulations. The results of the molecular dynamics simulations showed that flavanonols exhibited the highest stability among the test compounds, with an average root mean squared deviation of 0.139493 Å for anti-bacterial tests and 0.182499 Å for anti-inflammatory tests after 50 ns simulation. Based on the results of molecular dynamics simulations, in vitro anti-bacterial and anti-inflammatory testing was conducted using flavanonol compounds found in Ananas comosus plants. In the anti-bacterial test, the pineapple extract, at a 5% concentration, exhibited the largest inhibitory zone diameter, 3.53 mm. In the anti-inflammatory tests, the pineapple extract at an optimal concentration of 600 ppm showed the highest absorbance value for protein denaturation, measuring 0.11133 au.

***Keywords**: anti-bacteria, anti-inflammation, diabetic ulcer, in silico, in vitro*

ABSTRAK

Penelitian ini didorong oleh peningkatan jumlah pasien diabetes melitus yang diproyeksikan meningkat tiga kali lipat pada tahun 2030 dan potensi keanekaragaman hayati Indonesia yang sangat besar. Ulkus diabetikum merupakan salah satu komplikasi yang paling sering terjadi akibat diabetes melitus yang tidak terkontrol. Oleh karena itu, penelitian ini bertujuan untuk mengetahui potensi terapeutik keanekaragaman hayati Indonesia untuk mengatasi ulkus diabetikum, dengan fokus pada sifat anti bakteri dan anti inflamasi dari turunan metabolit sekunder, dengan menggunakan pendekatan in silico dan in vitro. Pada awalnya, penelitian ini menggunakan pendekatan in silico, dengan melakukan penambatan molekuler dan simulasi dinamika molekuler pada ligan referensi yang diperoleh dari reseptor 6KVS untuk bakteri *Staphylococcus aureus* dan 5KIR untuk protein COX-2. Docking molekuler dilakukan terhadap 18 senyawa uji turunan metabolit sekunder dengan menggunakan Autodock Vina, yang

***Received**: 18 December 2023* ***Accepted**: 13 September 2024* ***Published**: 16 November 2024*

dilanjutkan dengan simulasi dinamika molekuler. Hasil simulasi dinamika molekul menunjukkan bahwa flavanonol menunjukkan stabilitas tertinggi di antara senyawa uji, dengan rata-rata deviasi kuadrat rata-rata sebesar 0,139493 Å untuk uji anti bakteri dan 0,182499 Å untuk uji antiinflamasi setelah simulasi selama 50 detik. Berdasarkan hasil simulasi dinamika molekuler, dilakukan pengujian anti bakteri dan anti inflamasi secara in vitro dengan menggunakan senyawa flavanonol yang terdapat pada tanaman Ananas comosus. Pada uji anti bakteri, ekstrak nanas dengan konsentrasi 5% menunjukkan diameter zona hambat terbesar yaitu 3,53 mm. Pada uji anti inflamasi, ekstrak nanas pada konsentrasi optimal 600 ppm menunjukkan nilai absorbansi tertinggi untuk denaturasi protein, yaitu sebesar 0,11133 au.

Kata kunci: anti bakteri, anti inflamasi, tukak diabetik, in silico, in vitro

INTRODUCTION

Diabetes mellitus is indeed a chronic disease that poses a significant challenge to global health. In Indonesia alone, diabetes-related deaths reached a staggering 236,000 in 2021 (International Diabetes Federation 2021). This alarming number highlights the urgent need for effective prevention and treatment strategies to curb the rising tide of diabetes. Diabetes mellitus is an endocrine and metabolic disorder resulting from an overall insulin deficiency or defective insulin functioning. This disease causes numerous complications, one of the most common being diabetic ulcers. Diabetic ulcers, or neuropathic wounds, are a chronic complication of diabetes mellitus in the form of open wounds on the skin's surface due to blockages in blood vessels, which cause tissue necrosis. Diabetic ulcers are most commonly caused by microangiopathy, resulting in peripheral neuropathy, namely an uncontrolled increase in blood sugar, which causes vascular abnormalities and metabolic disorders in the affected nerves (Genco and Borgnakke 2020). If not appropriately controlled, diabetic ulcers can cause further acute complications such as cellulitis, neuropathy, abscesses and gangrene (Bolton 2018; Dorresteijn et al. 2014; Giacomozzi et al. 2018; Levy and Gillibrand 2019). Moreover, diabetic ulcers often trigger a chronic inflammatory response, characterized by the infiltration of immune cells and the release of inflammatory mediators. This persistent inflammation impedes wound healing and increases the risk of infection. Common bacterial pathogens associated with diabetic foot ulcers include *Staphylococcus aureus*, Pseudomonas aeruginosa, and Escherichia coli (Tiek Chiang Goh, 2020). Diabetic wounds can occur in any area of the human body, including the extremities. These wounds may exhibit a range of infections, from mild to severe, with some proving difficult to treat effectively (MM Martinez Delgado, 2018; Mohamed Abdulhammeed Hatem, 2022).

This study employs Computer-Aided Drug Design (CADD) to virtually screen potential medicinal plants to develop novel diabetic ulcer drugs that promote wound healing. CADD approaches offer a cost-effective and time-efficient method to identify drug candidates with inhibitory activity against COX-2, an enzyme responsible for excessive prostaglandin E_2 (PGE2) production in wound macrophages (Wang and Wang 2018), and *Staphylococcus aureus*, the most prevalent isolated pathogen in diabetic ulcer wounds (Dunyach-Remy et al. 2016). Molecular docking and virtual screening techniques will be employed, as these methods have successfully identified potential therapies for diabetic ulcers by evaluating protein-ligand binding energy (Hosseini et al. 2021). However, molecular docking is limited by protein flexibility, solvation models, and the simplicity of scoring functions (Souza et al. 2021). To ensure more reliable findings, molecular docking will be complemented by full atomistic molecular dynamics simulation, which examines the dynamic behavior of a ligand, protein, and solvent at a specific time (Santos et al. 2019). To further enhance the credibility of our simulations, in vitro anti-bacterial and anti-inflammatory assays will also be conducted to investigate the properties of bioactive compounds in

inhibiting *Staphylococcus aureus* and assessing their anti-inflammatory effects in protein BSA denaturation.

MATERIALS AND METHODS

In Silico Test

3D structures preparation

The 3D model protein structures of *Staphylococcus aureus* bacteria and human cyclooxygenase-2 (COX-2) used were OAX (4-chloranyl-N-[[cyclopropylmethyl(methanoyl)amino]methyl]benzamide) and RCX (rofecoxib), obtained from the RCSB Protein Data Bank (PDB) with accession codes 6KVS and 5KIR, respectively.

These structures were prepared using AutoDock Vina software for docking simulations. Water molecules were eliminated from the protein structures, and the respective reference ligands, OAX (PDB entry 6KVS) and RCX (PDB entry 5KIR) were extracted. OXA-1, a protein target, is a type of beta-lactamase enzyme that breaks down beta-lactam antibiotics, which helps bacteria develop resistance to antibiotics (International Journal of Medical Microbiology, 2018). OXA-1 proteins in *Staphylococcus aureus* are also responsible for assisting the assembly of several different substrate proteins (Nathalie, 2009). Identifying potential drug candidates capable of exhibiting inhibitory activity against cyclooxygenase-2 (COX-2) and *Staphylococcus aureus* is of significant interest. COX-2 is an enzyme responsible for excessive prostaglandin E_2 (PGE2) production in wound macrophages, while *Staphylococcus aureus* is the most commonly isolated pathogen in diabetic ulcer wounds. Rofecoxib, a medication used to inhibit COX-2 activity, is a ligand for this enzyme.

Polar hydrogens were added to the target proteins, nonpolar hydrogens were merged, and Gasteiger charges were assigned. The reference ligands were converted into the PDBQT format that is compatible with AutoDock Vina. Subsequently, secondary metabolite derivatives from plants with similar geometrical structures to the reference ligands were retrieved from PubChem for further investigation as potential COX-2 inhibitors.

Molecular docking

Molecular docking simulations were conducted using AutoDock Vina software on a laptop with an Intel® Core™ i5-7200U CPU, 16.0 GB RAM, Windows 10 64-bit operating system, and Intel® Iris® Plus Graphics GPU. The reference ligands, OAX and RCX, were redocked onto their respective target proteins to validate the docking method. Subsequently, all prepared secondary metabolites were subjected to molecular docking on the target proteins under parameters identical to those used for the reference ligands. The docking parameters for OAX were as follows: central grid point coordinates (10.829, 14.375, 1.652), grid box size 40 × 38 × 38, and grid point spacing 0.375 Å. The docking parameters for RCX were as follows: central grid point coordinates (23.287, 0.439, 34.435), grid box size 40 × 40 × 40, and grid point spacing 0.375 Å. Both molecular docking simulations employed default docking parameters using the Lamarckian Genetic Algorithm. The intermolecular forces formed during docking were analyzed using BIOVIA Discovery Studio 2021 Visualizer.

Molecular dynamics simulations

Molecular dynamics (MD) simulations were conducted using Amber20 software to assess the stability of the protein-ligand complex. The generated structure was incorporated into LEaP, adding water and an Mg^{+2} ion. Both water and the entire system were subjected to energy minimization. The resulting MD trajectories were analyzed using AmberTools20 to determine root-mean-square deviation (RMSD), which provides insights into the overall structural stability of the protein-ligand complex over time. Lower RMSD values indicate greater stability, suggesting a strong protein and ligand interaction.

Drug-likeness and absorption, distribution, metabolism, excretion, and toxicity (ADMET) prediction

The drug-likeness of the secondary metabolites was evaluated using Lipinski's rule of five, which was implemented on the SCFBio Lipinski website. This rule encompasses five criteria to determine whether a compound exhibits drug-like properties. To

be considered drug-like, a compound must have a molecular mass below 500 Da, a log P value less than 5, no more than five hydrogen bond donors, no more than ten hydrogen bond acceptors, a molar refractivity between 40-130 (m^3/mol), and not violate more than one of the five rules above. The pharmacokinetic properties, including absorption, distribution, metabolism, excretion, and toxicity (ADMET), were also predicted using the pkCSM server.

In Vitro Test

The experimental apparatus included autoclaves, blenders, analytical balances, spatulas, beakers, measuring cups, glass funnels, stirring rods, dropper pipettes, measuring flasks, Erlenmeyer flasks, mortar and pestles, cuvettes, test tubes, a water bath, a centrifuge, L-rods, Petri dishes, watch glasses, a Bunsen burner, pH indicators, tweezers, micropipettes, and laminar airflow cabinets. The materials required for the study included *Staphylococcus aureus* bacteria, bovine serum albumin, sodium phosphate dibasic heptahydrate (Na_2HPO_4), sodium phosphate monobasic monohydrate (NaH_2PO_4), sodium chloride (NaCl), potassium chloride (KCl), and pineapple (*Ananas comosus*).

The pineapple extract was prepared and evaluated for its antibacterial activity against *Staphylococcus aureus* using the agar diffusion method. The optimal concentration for the antibacterial effect was determined based on the inhibition zone diameter. Subsequently, the extract's anti-inflammatory potential was assessed by its ability to prevent protein denaturation, with the optimal concentration determined based on the minimum protein denaturation percentage.

RESULTS AND DISCUSSION

Anti-Bacterial Property Test

Molecular docking

In this method, the structure of the reference ligand obtained from molecular docking is overlaid onto the structure derived from the Protein Data Bank's (PDB) X-ray diffraction (XRD) data, the 3D Superimposition of Reference Ligand (OAX) structure is shown in Figure 1. The molecular docking simulations indicated that OAX, the reference ligand, exhibited a binding energy of -6.75 kcal/mol and an RMSD value of 0.96Å in Figure 2. The RMSD parameter is critical in validating the docking results through a re-docking procedure. The molecular docking outcome is deemed valid if the RMSD value falls within the acceptable threshold of ≤ 2Å. This RMSD value is a control parameter for evaluating the accuracy of docking various chemical compounds.

The size of the ligand search box was adjusted to encompass the complex formed between the receptor and the ligand by placing a search point at the box's coordinates (X, Y, and Z) that encloses the binding site region of the ligand. The grid box is where the ligand will interact with the amino acid residues of the target protein. The grid box is determined to identify the coordinate points in the binding area of a protein. In this study, the grid box size used was X (40), Y (38), and Z (38) with an X center (10.829), Y center (14.375), and Z center (1.652), which are presented in Figure 3. This data was used as a control variable for docking test compounds.

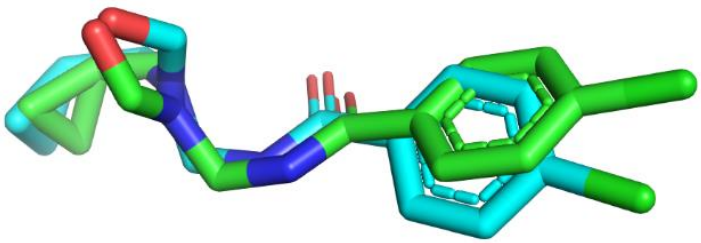

Figure 1. Superimposition of Reference Ligand (OAX).

Rank	Sub-Rank	Run	Binding Energy	Cluster RMSD	Reference RMSD
1	1	1	-6.75	0.00	0.96
1	2	4	-6.59	1.22	1.50
1	3	9	-6.59	1.00	1.29
2	1	3	-6.52	0.00	3.70
2	2	7	-6.37	1.79	4.03
2	3	6	-6.35	1.86	4.11
2	4	5	-6.33	1.87	3.87
2	5	8	-6.32	1.93	3.92
2	6	10	-6.31	1.87	3.84
3	1	2	-6.49	0.00	2.31

Figure 2. Root Mean Square Deviation And Binding Energy

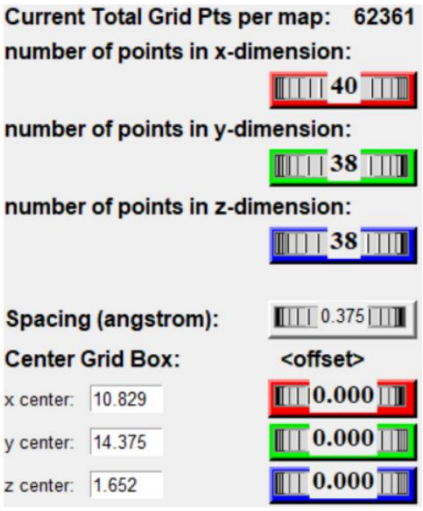

Figure 3. Grid Box Dimension of Molecular Docking Anti-Bacterial Property Test

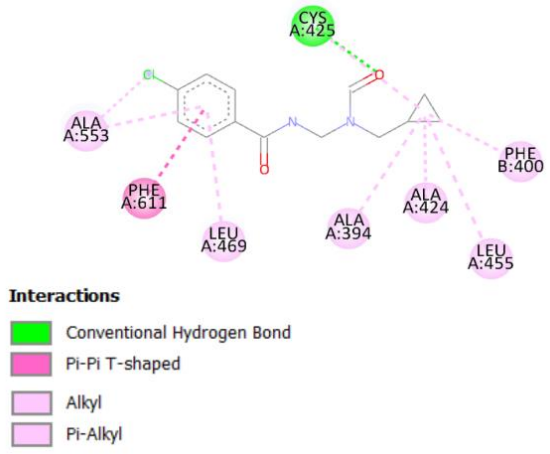

Figure 4. The 2D visualization of ligan-receptor

In drug discovery, compounds exhibiting more negative than positive control binding energies are regarded as promising drug candidates. This stems from the notion that a more negative binding energy reflects a stronger and more stable interaction between the receptor and the ligand, a crucial attribute for effective drug action. A stronger bond between the ligand and receptor sug-

gests that the ligand is less likely to dissociate from the receptor, prolonging its therapeutic effect. Therefore, compounds with more negative than positive control binding energies are prioritized for further investigation as potential drug candidates. The 2D visualization of the interaction between ligand and receptor is shown in Figure 4.

According to the molecular docking results, the three compounds with the best binding energy to *Staphylococcus aureus* prove to be chalcone, anthocyanin, and flavanonol with free Gibbs energy of -8.60 kcal/mol, -8.40 kcal/mol, and -8.10 kcal/mol respectively. The molecules were selected based on their structural similarity and the number of benzene rings chosen to match the characteristics of the target proteins, OAX and RCX. These compounds will be further analyzed through Lipinski's Rule of Five, Pre-ADMET simulations and molecular dynamics (Table 1).

Table 1. Molecular docking result.

Chemical compounds	Scientific name	Parts used	Binding energy (kcal/mol)
Reference ligand	-	-	-6.75
Chalcone	*Citrus reticulata*	Fruit Peel	-8.60
Anthocyanin	*Punica granatum*	Fruit	-8.40
Flavanonol	*Ananas comosus*	Fruit Peel	-8.10
Flavanone	*Citrus amblycarpa*	Fruit Peel	-8.10
Spiraeoside	*Allium cepa*	Bulb Peel	-8.10
Flavone	*Moringa oleifera*	Leaf	-7.90
Aurone	*Psophocarpus tetragonolobus*	Leaf	-7.80
Catechin	*Camellia sinensis*	Leaf	-7.80
Epicatechin	*Malus domestica*	Fruit Peel	-7.80
Naringin	*Citrus paradisi*	Seed	-7.80
Quercetin	*Zingiber officinale*	Leaf	-7.70
Daidzein	*Pueraria lobata*	Root	-7.60
Isoflavone	*Vitis vinifera*	Fruit	-7.50
Genistein	*Glycine max*	Seed	-7.40
Leucodelphidine	*Caesalpinia pulcherrima*	Stem	-7.30
Triclosan	*Daucus carota*	Tuber	-7.10
Acridine	*Citrus sinensis*	Fruit Peel	-7.00
Dihydrochalcone	*Glycyrrhiza glabra*	Root	-7.00

Molecular dynamics simulations

Root Mean Square Deviation (RMSD) measures how much a molecule's conformation changes during a molecular dynamics simulation. A lower RMSD value indicates that the compound is more stable, as an increase in RMSD value suggests that the protein structure begins to open up so that the ligand starts to search for binding sites on the protein.

Based on Figure 5 and Table 2, flavanonol has the best average RMSD value among other secondary metabolite derivatives and the reference ligand as a control. The reference ligand has a higher RMSD value due to being less stable than flavanonol, as it undergoes greater structural changes during the simulation. In comparison, flavanonol demonstrates smaller structural changes and more stable and rigid conformation with a lower RMSD value. Flavanonol has an average RMSD value of 0.139493 Å after 50 ns of molecular dynamics simulation. Thus, based on the RMSD simulation, flavanonol has a more significant potential than other secondary metabolite derivatives when assessed based on the RMSD value obtained.

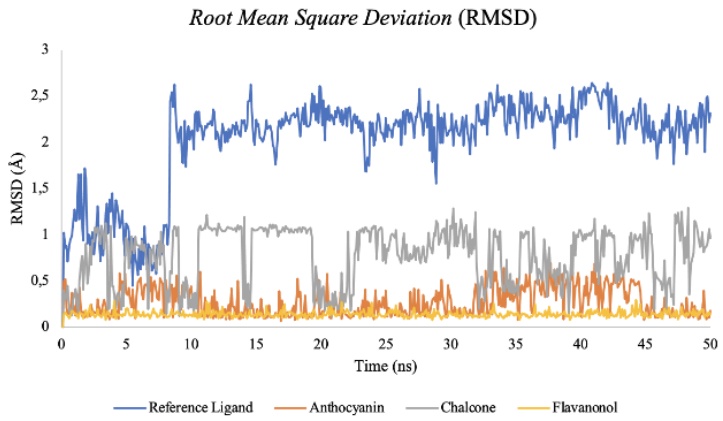

Figure 5. Root mean square deviation (RMSD) values of protein 6KVS for 50 ns.

Table 2. Average root mean square deviation (RMSD) values of protein 6KVS for 50 ns.

Secondary metabolite compounds	Average RMSD (Å) value
Reference Ligand	2.022598
Anthocyanin	0.266450
Chalcone	0.774259
Flavanonol	**0.139493**

Drug-likeness and ADMET prediction

Lipinski's Rule of Five testing is conducted to determine the potential of a drug candidate to become an oral drug. Based on the Lipinski rule for developing oral drug candidates, it must meet the "Rule of Five" conditions related to molecular weight, octanol-water coefficient value, number of hydrogen bond donors, number of hydrogen bond acceptors, and molar refraction. If a compound meets all regulations with a maximum of one violation, then the compound has the potential to be used as an oral drug. However, if the compound violates more than one regulation, the treatment can be through a non-oral route such as injection or topical (Table 3).

Table 3. Lipinski's rule of five tests.

Chemical compounds	Molecular mass (Dalton)	Hydrogen bond donors	Hydrogen bond acceptors	Octanol water partition coefficient (log P)	Molar refractivity (m^3/mol)	Number of violation
Parameter	≤ 500 (Da)	≤ 5	≤ 10	0 ≤ log P ≤ 5	40-130 (m^3/mol)	≯ 1
Reference Ligand (OAX)	251.5	0	3	-0.062600	54.525898	1
Chalcone	208.0	0	1	3.582699	66.248482	0
Anthocyanin	207.0	0	1	4.190880	65.395988	0
Flavanonol	240.0	1	3	2.363900	66.590286	0

*The red colour indicates that the chemical compound does not meet the criteria of the corresponding parameter

An assessment of the structural properties of the synthesized compounds using Lipinski's Rule of Five revealed their potential for oral bioavailability. This rule dictates

that orally active drugs should adhere to specific physicochemical parameters, including a molecular weight less than 500 Dalton, a maximum of five hydrogen bond donors and ten hydrogen bond acceptors, an octanol-water partition coefficient (log P) not exceeding 5, and a molar refractivity index between 40 and 130 m^3/mol. These parameters influence the drug's ability to penetrate biological membranes, dissolve in physiological fluids, and interact with cellular targets. All compounds in this study complied with Lipinski's Rule of Five, suggesting their suitability for oral administration.

Following the assessment of compound characteristics using Lipinski's Rule of Five, the next step involves conducting Pre-Absorption Distribution Metabolism Excretion (Pre-ADMET) studies. Pre-ADMET evaluations aim to predict the pharmacokinetic and toxicological properties of candidate compounds. These studies provide valuable insights into compounds' potential drug-likeness and safety profile, guiding further optimization and development efforts.

Absorption test analysis

The absorption potential of candidate drug compounds was evaluated by determining their intestinal absorption and skin permeability. The results indicated that all compounds exhibited high intestinal absorption, exceeding 80%. In contrast, the reference ligand and flavanonol demonstrated favorable skin permeability, with values of -2.946 log Kp and -2.918 log Kp, respectively. A more negative skin permeability value signifies a higher ability of the drug compound to permeate the skin and enter the body through transdermal absorption. The pharmacokinetic profile for the absorption test analysis is shown in Table 4.

Table 4. The pharmacokinetic profile of the absorption test analysis with reference ligand OAX

Chemical Compounds	Water Solubility	$Caco_2$ Permeability	Intestinal Absorption (%)	Skin Permeability	P-glycoprotein substrate	P-glycoprotein I inhibitor	P-glycoprotein II inhibitor
Parameter	> -4	> 0.9	> 80%	< -2.5	Negative	Negative	Negative
Reference Ligand (OAX)	-3.701	1.288	97.825	-2.946	Positive	Negative	Negative
Chalcone	-4.461	1.335	94.977	-1.998	Positive	Negative	Negative
Anthocyanin	-4.852	1.631	96.182	-2.128	Negative	Negative	Negative
Flavanonol	-3.266	1.227	94.820	-2.918	Positive	Negative	Negative

*The red colour indicates that the chemical compound does not meet the criteria of the corresponding parameter

Distribution test analysis

The distribution of the tested compounds was assessed using two main parameters: volume of distribution (VDss) and blood-brain barrier (BBB) permeability. VDss represents the theoretical volume in which the total drug dose would need to be evenly distributed to achieve the same concentration as in blood plasma. Chalcone exhibited the best distribution profile, with a VDss value of 0.365 log L/kg. However, this value is still considered low for overall distribution in the body. All compounds, except the reference ligand, could penetrate the BBB effectively, as indicated by log BB values exceeding 0.3 log BB.

Metabolism test analysis

The metabolism assessment specifically focused on CYP2D6 substrate-inhibitor activity. Cytochrome P450 is a prevalent detoxification enzyme found in the liver and plays a crucial role in metabolizing foreign substances through oxidation. Inhibiting cytochrome P450 enzymes can potentially interfere with drug metabolism, making it essential to evaluate the inhibitory potential of compounds on CYP2D6. The CYP2D6 substrate-inhibitor activity test results revealed that none of the tested compounds exhibited inhibitory or modulatory effects on the CYP2D6 enzyme.

Excretion test analysis

Total clearance (CLTOT) and renal organic cation transporter 2 (OCT2) substrate activity are two critical parameters for predicting the excretion process of a compound. CLTOT represents the combined effect of hepatic clearance (metabolic breakdown in the liver and bile) and renal clearance (excretion through the kidneys). This parameter is crucial for determining bioavailability and establishing appropriate dosage levels to achieve therapeutic concentrations. The CLTOT values of the tested compounds range from 0.006 to 0.716, indicating varying degrees of elimination efficiency. None of the tested compounds also demonstrated an effect on OCT2 substrate transport, suggesting that they are not substrates for this transporter. OCT2 plays a significant role in the clearance of drugs and endogenous compounds, and its inhibition can lead to potential adverse effects. Therefore, the absence of OCT2 interaction is an advantageous property for these compounds.

Toxicity test analysis

The toxicological properties of the test compounds were evaluated using Ames Toxicity, LD_{50}, and Maximum Tolerated Dose (MTD) tests. Flavanonol was the only compound with positive results in the Ames test, indicating its potential mutagenic properties and carcinogenic activity. Based on the LD_{50} classification, the reference ligand belongs to GHS toxicity class 5, which signifies low acute toxicity, while all other compounds fall within GHS toxicity class 4. According to the toxicity classification scheme proposed by Hodge and Sterner, all compounds at the tested doses belong to toxicity class 4, indicating relatively low toxicity. Chalcone demonstrated the highest MTD value (1.031 log mg/kg/day) among the test compounds, suggesting that it can be consumed in the highest amount compared to the other compounds.

In vitro test

In vitro, antibacterial testing was performed to identify the most effective compound. Based on the root mean square deviation (RMSD) values obtained from molecular dynamics simulations of 50 ns, flavanonol exhibited a more stable average RMSD than other test compounds. Therefore, antibacterial testing was performed against flavanonol, a compound found in pineapple (*Ananas comosus*), with the following results in Figure 6 and Figure 7.

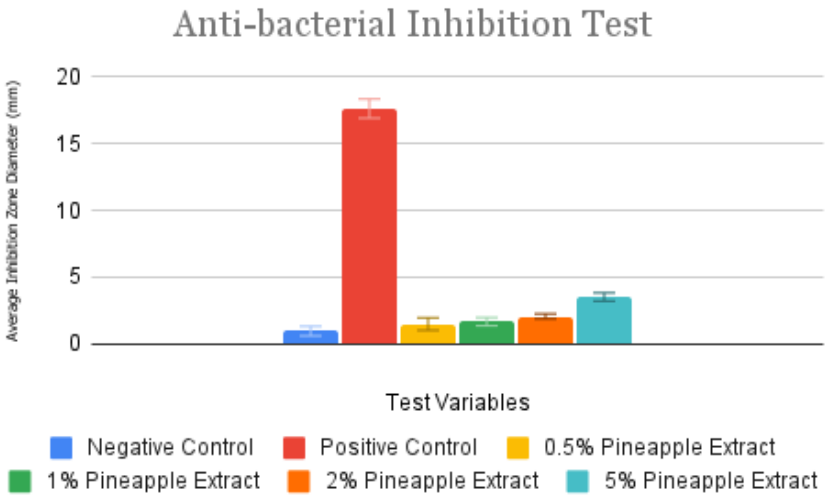

Figure 6. Inhibition zone diameter of *Staphylococcus aureus* bacteria.

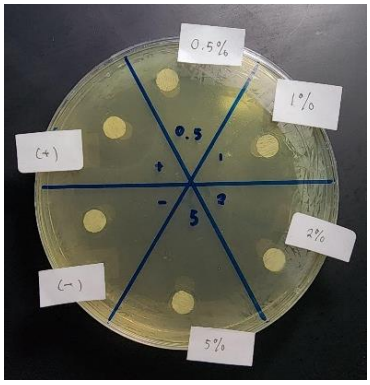

Figure 7. Inhibition zone diameter of test variables against *Staphylococcus aureus*.

Pineapple extract containing flavanonol exhibited antibacterial activity against *Staphylococcus aureus* bacteria. This activity was concentration-dependent, with higher concentrations leading to larger inhibition zones. Spearman's rank correlation coefficient ($r = 0.999$; $p = 0.00145$) indicated a strong positive correlation between extract concentration and inhibition zone diameter, which supports this observation.

However, the inhibitory potency of pineapple extract was still classified as weak compared to the antibiotic amoxicillin. According to the established criteria for inhibition strength (Silaban 2021), amoxicillin falls under the strong category with an inhibition zone of 17.6 mm, while a 5% pineapple extract concentration only produced an inhibition zone of 3.53 mm. Additionally, the phosphate buffer alone demonstrated a minimal inhibitory effect of 0.96 mm, suggesting some antibacterial activity may be attributed to the buffer. Further investigation is warranted to elucidate the underlying mechanism of action and identify the specific active compounds within the extract.

Despite its weak inhibitory effect, flavanonol is a promising candidate for further development as an antibacterial agent. Its structural stability, as indicated by the RMSD values, suggests that it is less likely to degrade or undergo conformational changes in the presence of bacteria. This could make it a more effective antibacterial agent than other less stable compounds.

Flavanonol, a flavonoid derivative, is a polyphenolic compound with known antibacterial properties, primarily mediated by the inhibition of nucleic acid synthesis (Cushnie and Lamb 2005). Flavonoid secondary metabolites can intercalate or form hydrogen bonds with nucleic acid bases, hindering the formation of crucial enzymes involved in cell replication, such as DNA gyrase. However, the hydroxyl group at the 3' position of the C ring in flavanonol has been shown to diminish DNA gyrase inhibition activity in *Escherichia coli* (Shamsudin et al. 2022). This observation aligns with flavanonol-containing pineapple extract's relatively weak antibacterial activity against *Staphylococcus aureus*. Further research must delve into flavanonol's chemical structure-activity relationships and precise inhibition mechanisms, particularly the impact of the 3' hydroxyl group modification.

Anti-Inflammatory Property Test
Molecular docking

Molecular docking simulations were conducted to assess the binding energy and interactions of RCX, the reference ligand, with the target protein. The docking results indicated that RCX exhibited a favorable binding energy of -10.78 kcal/mol and an RMSD value of 1.27 Å are shown in Figure 8. The RMSD parameter is crucial in validating the docking results through a re-docking procedure. In this method, the structure of the reference ligand obtained from molecular docking is overlaid onto the structure derived from the Protein Data Bank's (PDB) X-ray diffraction (XRD) data, the 3D Superimposition of Reference Ligand (RCX) structure is shown in Figure 9. The molecular docking outcome is considered valid if the RMSD value falls within the acceptable threshold of ≤ 2Å. This RMSD value is a control parameter for evaluating the accuracy of docking various chemical compounds. A low

RMSD value indicates that the docked pose closely resembles the actual binding mode of the ligand, providing strong support for the reliability of the docking results.

The ligand search box dimensions were optimized to include the receptor-ligand complex by establishing a search point at the coordinates (X, Y, Z) corresponding to the ligand's binding site region. This grid box defines the area where the ligand interacts with the amino acid residues of the target protein. Determining the grid box is crucial for identifying the coordinate points within a protein's binding region. In this study, the grid box was set to a size of 40, with center coordinates at X (23.287), Y (0.439), and Z (34.435) in Figure 10. These coordinates were utilized as a control variable for the docking of test compounds.

Rank	Sub-Rank	Run	Binding Energy	Cluster RMSD	Reference RMSD
1	1	9	-10.79	0.00	1.27
1	2	3	-10.78	0.06	1.29
1	3	8	-10.78	0.05	1.27
1	4	1	-10.78	0.05	1.27
1	5	7	-10.77	0.08	1.25
1	6	6	-10.77	0.04	1.27
1	7	5	-10.76	0.16	1.26
1	8	10	-10.75	0.12	1.23
1	9	4	-10.73	0.17	1.25
1	10	2	-10.72	0.14	1.25

Figure 8. Root Mean Square Deviation And Binding Energy.

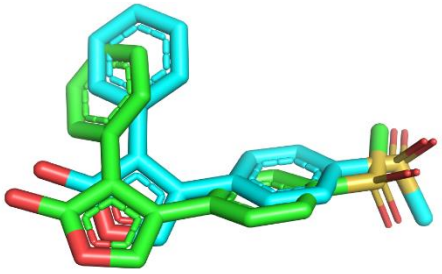

Figure 9. Superimposition of reference ligand (RCX).

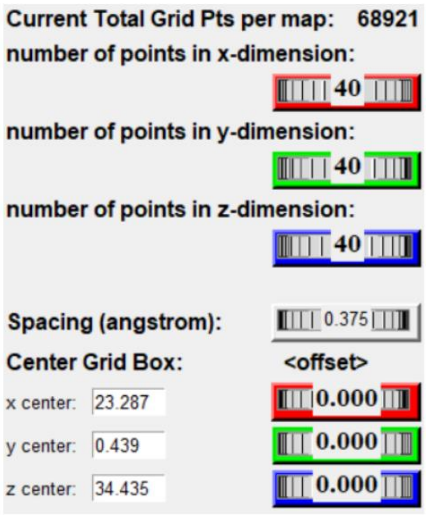

Figure 10. Grid box dimension of *molecular docking anti-inflammatory property test*.

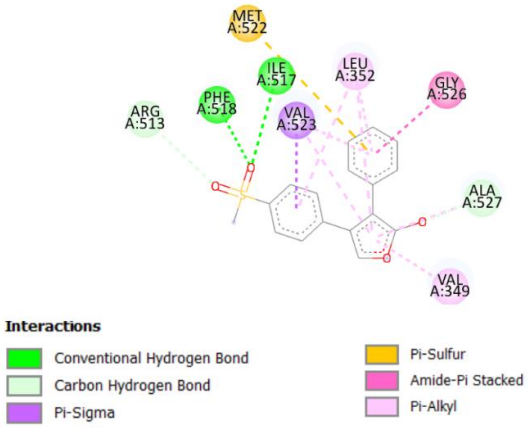

Figure 11. The 2D Visualization of Ligan-Receptor.

In drug discovery, compounds exhibiting more negative than positive control binding energies are considered promising drug candidates (Kar et al. 2022; Terefe EM, Ghosh 2022). This preference stems from the understanding that a more negative binding energy signifies a stronger and more stable interaction between the receptor and the ligand. Such a robust interaction is considered crucial for effective drug action. A stronger bond between the ligand and the receptor implies a lower likelihood of ligand dissociation, leading to a prolonged therapeutic effect. Consequently, compounds with more negative than positive control binding energies are prioritized for further investigation as potential drug candidates. The 2D visualization of the interaction between ligand and receptor is shown in Figure 11.

The molecular docking results revealed that spiraeoside, isoflavone, and flavanonol exhibited the most favorable binding energies towards COX-2, with free Gibbs energies of -9.20 kcal/mol, -9.20 kcal/mol, and -9.80 kcal/mol, respectively. These promising compounds will be evaluated using Lipinski's Rule of Five, Pre-ADMET simulations, and molecular dynamics to assess their drug-likeness and potential pharmacokinetic properties (Table 5).

Table 5. Molecular docking result.

Chemical compounds	Scientific name	Parts used	Binding energy (kcal/mol)
Reference Ligand	-	-	-10.78
Flavanonol	*Ananas comosus*	Fruit Peel	-9.80
Isoflavone	*Vitis vinifera*	Fruit	-9.20
Spiraeoside	*Allium cepa*	Bulb Peel	-9.20
Flavone	*Moringa oleifera*	Leaf	-9.00
Leucodelphidine	*Caesalpinia pulcherrima*	Stem	-8.90
Naringenin	*Citrus paradisi*	Seed	-8.80
Anthocyanin	*Punica granatum*	Fruit	-8.80
Chalcone	*Citrus reticulata*	Fruit Peel	-8.60
Aurone	*Psophocarpus tetragonolobus*	Leaf	-8.60
Flavanone	*Citrus amblycarpa*	Fruit Peel	-8.50
Epicatechin	*Malus domestica*	Fruit Peel	-8.40
Catechin	*Camellia sinensis*	Leaf	-8.40
Quercetin	*Zingiber officinale*	Leaf	-8.30
Genistein	*Glycine max*	Seed	-8.30
Dihydrochalcone	*Glycyrrhiza glabra*	Root	-8.20
Acridine	*Citrus sinensis*	Fruit Peel	-8.10
Triclosan	*Daucus carota*	Tuber	-8.10
Daidzein	*Pueraria lobata*	Root	-8.00

Molecular dynamics simulations

Flavanonol exhibits the most favorable average RMSD value among the secondary metabolite derivatives and the reference ligand, demonstrating remarkable stability during the 50ns molecular dynamics simulation. Its average RMSD value of 0.182499 Å suggests superior stability compared to other derivatives, making it a promising candidate for further investigation through an *in vitro* approach in Figure 12 and Table 6.

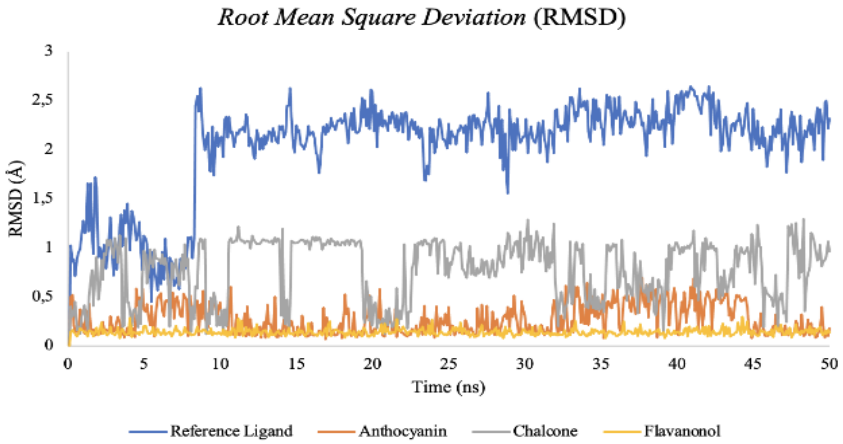

Figure 12. Root mean square deviation (RMSD) values of protein 5KIR for 50 ns.

Table 6. Average root mean square deviation (RMSD) values of protein 5KIR for 50 ns.

Secondary metabolite compounds	Average RMSD (Å) value
Reference Ligand	0.249083
Flavanonol	**0.182499**
Isoflavone	0.186032
Spiraeoside	1.356695

Drug-likeness and ADMET prediction

The application of Lipinski's Rule of Five revealed that only isoflavone and flavanonol among the three compounds exhibit characteristics favorable for oral bioavailability (Benet et al. 2016; Choy and Prausnitz 2011). According to this rule, molecular weight plays a crucial role in determining the absorption potential of a drug. Compounds with molecular weights exceeding 500 Da may face challenges penetrating biological membranes, leading to delayed absorption. Additionally, the number of hydrogen bond donors and acceptors significantly impacts physicochemical properties such as melting point, solubility, and chelation ability. Spiraeoside fails to meet the criteria for hydrogen bond donors and acceptors, with eight hydrogen bond donors and 12 hydrogen bond acceptors. Furthermore, the octanol-water partition coefficient (log P) is a critical factor influencing drug absorption. A log P value greater than 5 indicates increased lipophilicity, potentially hindering absorption. Conversely, compounds with highly negative log P values may exhibit poor solubility in lipid bilayer membranes, further impeding their ability to permeate these barriers. Finally, molar refractivity measures the polarizability of a drug molecule and should fall within the range of 40-130 m^3/mol according to Lipinski's Rule of Five. Based on these criteria, spiraeoside is deemed unsuitable for oral administration due to its violation of multiple Lipinski's Rule of Five parameters (Table 7).

Table 7. Lipinski's rule of five tests.

Chemical compounds	Molecular mass (Dalton)	Hydrogen bond donors	Hydrogen bond acceptors	Octanol Water partition coefficient (log P)	Molar refractivity (m^3/mol)	Number of violation
Parameter	≤ 500 (Da)	≤ 5	≤ 10	0 ≤ log P ≤ 5	40-130 (m^3/mol)	⊁ 1
Reference Ligand (RCX)	300	0	4	0	0	1
Flavanonol	240	1	1	2.363900	66.590286	0
Isoflavone	222	0	1	3.302799	65.819489	0
Spiraeoside	464	8	12	0.781600	106.184853	2

*The red colour indicates that the chemical compound does not meet the criteria of the corresponding parameter

Absorption test analysis

The absorption potential of drug candidate compounds was evaluated by assessing their intestinal absorption and skin permeability. Based on intestinal absorption data, Spiraeoside exhibited an absorption value below 80%, indicating poor intestinal uptake. Conversely, skin permeability results revealed that the reference ligand, flavanonol, and spiraeoside demonstrated favorable skin permeability values of -2.946 log Kp, -2.918 log Kp, and -2.735 log Kp, respectively. A lower skin permeability value indicates a higher ability of the drug compound to permeate the skin and enter the body via topical administration (Yu et al. 2021). The pharmacokinetic profile for the absorption test analysis is shown in Table 8.

Table 8. The pharmacokinetic profile of the absorption test analysis with reference ligand RCX

.

Chemical Compounds	**Water Solubility**	**$Caco_2$ Permeability**	**Intestinal Absorption (%)**	**Skin Permeability**	**P-glycoprotein substrate**	**P-glycoprotein I inhibitor**	**P-glycoprotein II inhibitor**
Parameter	> -4	> 0.9	> 80%	< -2.5	Negative	Negative	Negative
Reference Ligand (RCX)	-4.217	1.289	98.413	-2.717	Negative	Negative	Negative
Flavanonol	-3.266	1.227	94.820	-2.918	Positive	Negative	Negative
Isoflavone	-4.351	1.767	96.388	-2.205	Positive	Negative	Positive

Distribution test analysis

Regarding drug distribution, we examined the volume of distribution (VDss) and blood-brain barrier (BBB) permeability. The VDss value represents the theoretical volume in which the entire drug dose must be evenly distributed to achieve the same concentration as in blood plasma. Spiraeoside exhibited the most favorable distribution volume, with a value of 1.999 log L/kg. According to BBB permeability results, spiraeoside is the only compound with limited brain penetration due to its log BB value being less than -1.

Metabolism test analysis

The metabolism assessment explicitly centred on the effect of the test compounds on CYP2D6 substrate-inhibitor activity. Inhibiting cytochrome P450 enzymes can potentially disrupt drug metabolism, making it crucial to assess the inhibitory potential of compounds on CYP2D6. Based on the CYP2D6 substrate-inhibitor activity results, none of the test compounds exhibited any inhibitory or interfering effects on the CYP2D6 enzyme.

Excretion test analysis

Clearance (CLTOT) and OCT2 substrate activity are crucial for predicting drug excretion. CLTOT values range from 0.006 to 0.888 in the tested compounds. None of the compounds interact with OCT2, suggesting they are not substrates. Additionally, no effect on OCT2 transport was observed. The absence of OCT2 interaction is advantageous for these compounds.

Toxicity test analysis

The toxicity of the test compounds was evaluated through Ames Toxicity, LD_{50}, and Maximum Tolerated Dose (MTD) assessments. The Ames test results indicate that the reference ligand and flavanonol exhibit positive mutagenicity, suggesting a potential for carcinogenic properties. LD50 classification reveals that the reference ligand and spiraeoside fall under GHS toxicity class 5, implying low acute toxicity. In contrast, all other compounds belong to GHS toxicity class 4. When analyzed using the Hodge and Sterner toxicity class tabulation, all compounds fall under toxicity class 4 at the tested dose, indicating relatively low toxicity. Among the test compounds, flavanonol exhibits the highest MTD value of 0.98 log mg/kg/day, indicating the highest tolerable dose.

In vitro test

The anti-inflammatory potential of flavanonol was evaluated *in vitro* following the identification of promising candidates through *in silico* screening. Molecular dynamics simulations assessed the conformational stability of flavanonol and other test compounds over a 50 ns timeframe. Flavanonol exhibited a more stable RMSD profile than the different compounds, suggesting enhanced structural integrity. The anti-inflammatory activity of flavanonol was further validated *in vitro* using sodium diclofenac as a positive control in Figure 13.

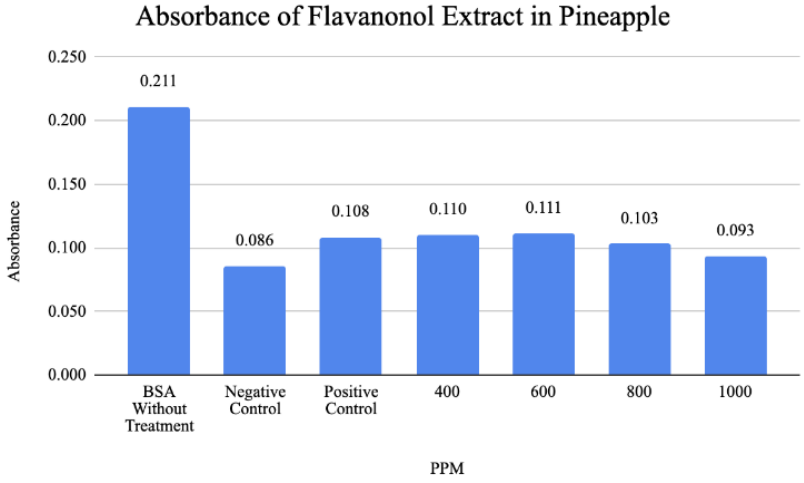

Figure 13. The absorbance of pineapple extract.

The anti-inflammatory efficacy of the pineapple flavanonol extract peaked at a concentration of 600 ppm, as evidenced by the highest average absorbance value (0.11133 au) among all tested concentrations, surpassing even the positive control group. This finding suggests that the 600 ppm concentration of pineapple flavanonol holds significant promise as a potential anti-inflammatory drug due to its ability to prevent protein denaturation. The 400 ppm concentration also exhibited promising anti -inflammatory potential, as its absorbance value exceeded that of the positive control group. Despite the modest difference in absorbance values (approximately 0.002 au), the effectiveness of the 400 ppm concentration of pineapple flavanonol as an anti-inflammatory agent remains noteworthy.

The IC_{50} value of pineapple extract, determined using the linear regression equation between log concentration (X) and percentage inhibition (Y) in Figure 14, was calculated to be 2.9271 µg/ml. This IC_{50} value falls within the classification of strong compounds, indicating that a relatively low

concentration of pineapple flavanonol can effectively prevent protein denaturation. Consequently, flavonoid compounds in pineapple are considered potent anti-inflammatory agents with therapeutic potential.

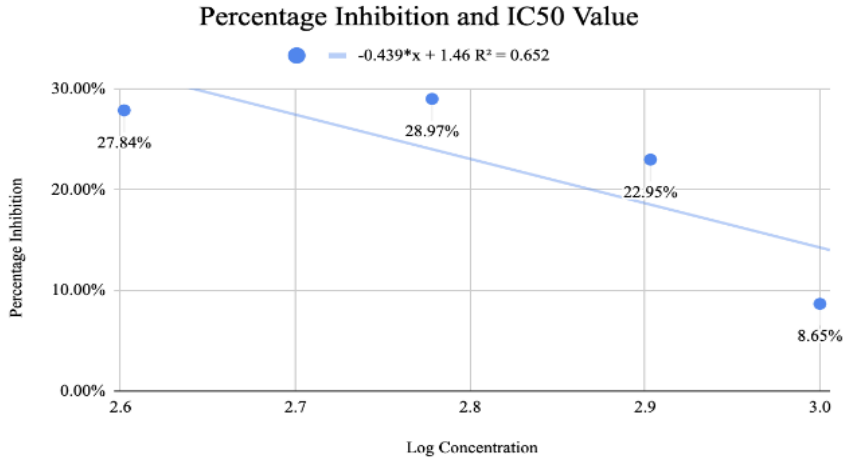

Figure 14. Percentage inhibitions and IC_{50} value.

Pineapple extract harbors flavonoid compounds, a versatile group of molecules with the potential to serve as the foundation for therapeutic agents targeting diverse chronic diseases. Among the secondary metabolite derivatives of flavonoids is flavanonol, a compound exhibiting pharmacological properties, notably anti-inflammatory activity. The multifaceted biological activities of flavonoids stem from their phenolic structure (Ginwala et al. 2019; Kumar and Pandey 2013; Rupasinghe 2020; Ullah et al. 2020). The anti-inflammatory effects of flavonoid compounds are attributed to their ability to inhibit cyclooxygenase and lipoxygenase pathways and suppress histamine and leukocyte accumulation. Further, flavonoids can contribute to the anti-inflammatory process by hindering the secretion of arachidonic acid and lysosomal enzymes (Al-Khayri et al. 2022; Vezza et al. 2016). The limitations faced in this study were specifically the extraction of flavanonol secondary metabolites to achieve more optimal results. Conducting phytochemical analysis on the negative control and pineapple extract to identify the best test compound for actively inhibiting *Staphylococcus aureus* bacteria growth and protein-denaturing abilities.

CONCLUSION

Among the 18 secondary metabolite derivatives evaluated using *in silico* assays, flavanonol from pineapple extract emerged as the most promising antibacterial and anti-inflammatory agent. Molecular dynamics simulations confirmed flavanonol's stability in acting as a ligand for targeted proteins OAX in *Staphylococcus aureus* bacteria and RCX in human COX-2 enzyme. Antibacterial *in vitro* testing revealed a positive correlation between flavanonol concentration against bacterial growth inhibition. Additionally, flavanonol demonstrates high anti-inflammatory activity as it can inhibit protein denaturation, a key step in the inflammatory process.

ACKNOWLEDGEMENT

We sincerely thank the Scripps Research Institute, PubChem, Protein Data Bank, pkCSM online tools, Dassault Systems, and GROMACS for their invaluable contributions to this research. Their generous provision of the AutoDock software, chemical compounds database, protein database, Pre-ADMET software, Biovia Discovery Studio software, and molecular dynamics simulation software enabled us to conduct our research with the necessary resources and tools.

REFERENCES

Al-Khayri JM, Sahana GR, Nagella P, Joseph BV, Alessa FM, Al-Mssallem MQ (2022) Flavonoids as potential anti-inflammatory molecules: a review.

Molecules 27(9):2901. doi: 10.3390/molecules27092901.

Benet LZ, Hosey CM, Ursu O, Oprea TI (2016) BDDCS, the Rule of 5 and drugability. Adv Drug Deliv Rev 101:89-98. doi: 10.1016/j.addr.2016.05.007.

Bolton L (2018) Managing patients with diabetic foot ulcers. Wounds ;30(12):380-381.

Choy YB, Prausnitz MR (2011) The rule of five for non-oral routes of drug delivery: ophthalmic, inhalation and transdermal. Pharm Res 28(5):943-8. doi: 10.1007/s11095-010-0292-6.

Cushnie TP, Lamb AJ (2005) Antimicrobial activity of flavonoids. Int J Antimicrob Agents 26(5):343-56. doi: 10.1016/j.ijantimicag.2005.09.002.

Dorresteijn JA, Kriegsman DM, Assendelft WJ, Valk GD (2014) Patient education for preventing diabetic foot ulceration. Cochrane Database Syst Rev 2014(12):CD001488. doi: 10.1002/14651858.CD001488.pub5.

Dunyach-Remy C, Ngba Essebe C, Sotto A, Lavigne JP (2016) *Staphylococcus aureus* toxins and diabetic foot ulcers: role in pathogenesis and interest in diagnosis. Toxins 8(7):209. doi: 10.3390/toxins8070209.

Genco RJ, Borgnakke WS (2020) Diabetes as a potential risk for periodontitis: association studies. Periodontol 2000 83(1):40-45. doi: 10.1111/prd.12270. PMID: 32385881.

Giacomozzi C, Sartor CD, Telles R, Uccioli L, Sacco ICN (2018) Ulcer-risk classification and plantar pressure distribution in patients with diabetic polyneuropathy: exploring the factors that can lead to foot ulceration. Ann Ist Super Sanita 54(4):284-293. doi: 10.4415/ANN_18_04_04.

Ginwala R, Bhavsar R, Chigbu DI, Jain P, Khan ZK (2019) Potential role of flavonoids in treating chronic inflammatory diseases with a special focus on the anti-inflammatory activity of apigenin. Antioxidants 8(2):35. doi: 10.3390/antiox8020035.

Goh, T. C., Bajuri, M. Y., C. Nadarajah, S., Abdul Rashid, A. H., Baharuddin, S., & Zamri, K. S. (2020). Clinical and bacteriological profile of diabetic foot infections in a tertiary care. Journal of Foot and Ankle Research, 13(1). doi:10.1186/s13047-020-00406-y

Hatem, Mohamed Abdulhameed., Kamal, Dhafer M., Yusuf, Khalifa Abdulrahman (2022). Diabetic foot limb threatening infections: Case series and management review. IJS Open 48():p 100568, November 2022. doi: 10.1016/j.ijso.2022.100568.

Hosseini M, Chen W, Xiao D, Wang C (2021) Computational molecular docking and virtual screening revealed promising SARS-CoV-2 drugs. Precis Clin Med 4(1):1-16. doi: 10.1093/pcmedi/pbab001.

International Diabetes Federation (2021) IDF diabetes atlas, 10th edition. Brussels, Belgium: International Diabetes Federation.

Kar P, Kumar V, Vellingiri B, Sen A, Jaishee N, Anandraj A, Malhotra H, Bhattacharyya S, Mukhopadhyay S, Kinoshita M, Govindasamy V, Roy A, Naidoo D, Subramaniam MD (2022) Anisotine and amarogentin as promising inhibitory candidates against SARS-CoV-2 proteins: a computational investigation. J Biomol Struct Dyn 40(10):4532-4542. doi: 10.1080/07391102.2020.1860133.

Kumar S, Pandey AK (2013) Chemistry and biological activities of flavonoids: an overview. ScientificWorldJournal 2013:162750. doi: 10.1155/2013/162750.

Levy N, Gillibrand W (2019) Management of diabetic foot ulcers in the community: an update. Br J Community Nurs 24(Sup3):S14-S19. doi: 10.12968/bjcn.2019.24.Sup3.S14.

Martínez Delgado M. M. (2018). Clinical case: complicated diabetic foot ulcer. *Revista espanola de sanidad penitenciaria*, *20*(3), 121–124.

Rupasinghe HPV (2020) Special issue "flavonoids and their disease prevention and treatment potential": recent advances and future perspectives. Molecules 25(20):4746. doi: 10.3390/molecules25204746.

Santos LHS, Ferreira RS, Caffarena ER (2019) Integrating molecular docking and molecular dynamics simulations.

Methods Mol Biol 2053:13-34. doi: 10.1007/978-1-4939-9752-7_2.

Shamsudin NF, Ahmed QU, Mahmood S, Ali Shah SA, Khatib A, Mukhtar S, Alsharif MA, Parveen H, Zakaria ZA (2022) Antibacterial effects of flavonoids and their structure-activity relationship study: a comparative interpretation. Molecules 27(4):1149. doi: 10.3390/molecules27041149.

Silaban H (2021) The effect of various concentrations of ethanol extract of the leaves of *Paederia foetida* L. on the growth of *Escherichia coli* bacteria. JDDT 11(6):61-7. doi: 10.22270/jddt.v11i6.5037 .

Souza PCT, Limongelli V, Wu S, Marrink SJ, Monticelli L (2021) Perspectives on high-throughput ligand/protein docking with Martini MD simulations. Front Mol Biosci 8:657222. doi: 10.3389/fmolb.2021.657222.

Terefe EM, Ghosh A (2022) Molecular docking, validation, dynamics simulations, and pharmacokinetic prediction of phytochemicals isolated from *Croton dichogamus* against the HIV-1 reverse transcriptase. Bioinform Biol Insights 16:11779322221125605. doi: 10.1177/11779322221125605.

Ullah A, Munir S, Badshah SL, Khan N, Ghani L, Poulson BG, Emwas AH, Jaremko M (2020) Important flavonoids and their role as a therapeutic agent. Molecules 25(22):5243. doi: 10.3390/molecules25225243.

Vezza T, Rodríguez-Nogales A, Algieri F, Utrilla MP, Rodriguez-Cabezas ME, Galvez J (2016) Flavonoids in inflammatory bowel disease: a review. Nutrients 8(4):211. doi: 10.3390/nu8040211.

Wang W, Wang J (2018) Toll-like receptor 4 (TLR4)/Cyclooxygenase-2 (COX-2) regulates prostate cancer cell proliferation, migration, and invasion by NF-κB activation. Med Sci Monit 24:5588-5597. doi: 10.12659/MSM.906857.

Yu YQ, Yang X, Wu XF, Fan YB (2021) Enhancing permeation of drug molecules across the skin via delivery in nanocarriers: novel strategies for effective transdermal applications. Front Bioeng Biotechnol 9:646554. doi: 10.3389/fbioe.2021.646554.